Constraints on Dike Propagation from Continuous GPS Measurements

Paul Segall, Peter Cervelli

Department of Geophysics, Stanford University, Stanford, CA 94305.

Susan Owen

Department of Earth Sciences, University of Southern California, Los Angeles, CA 90089-0740

Mike Lisowski

Cascade Volcano Observatory, Vancouver, WA.

Asta Miklius

Hawaiian Volcano Observatory, Hawaii Volcanos National Park, HI.

Short title: DIKE PROPAGATION

Abstract.

The January 1997 East Rift Zone eruption on Kilauea volcano, Hawaii, occurred within a network of continuous Global Positioning System (GPS) receivers. The GPS measurements reveal the temporal history of deformation during dike intrusion, begining ~ 8 hours prior to the onset of the eruption. The dike volume as a function of time, estimated from the GPS data using elastic Green's functions for a homogeneous half-space, shows that only two thirds of the final dike volume accumulated prior to the eruption and the rate of volume change decreased with time. These observations are inconsistent with simple models of dike propagation, which predict accelerating dike volume up to the time of the eruption and little or no change thereafter. Deflationary tilt changes at Kilauea summit mirror the inferred dike volume history, suggesting that the rate of dike propagation is limited by flow of magma into the dike. A simple, lumped parameter model of a coupled dike magma-chamber system shows that the tendency for a dike to end in an eruption (rather than intrusion) is favored by high initial dike pressures, compressional stress states, large, compressible magma reservoirs, and highly conductive conduits linking the dike and source reservoirs. Comparison of model predictions to the observed dike volume history, the ratio of erupted to intruded magma, and the deflationary history of the summit magma chamber suggest that most of the magma supplied to the growing dike came from sources near to the eruption through highly conductive conduits. Interpretation is complicated by the presence of multiple source reservoirs, magma vesiculation and cooling, as well as spatial variations in dike-normal stress. Reinflation of the summit magma chamber following the eruption was measured by GPS and accompanied a rise in the level of the Pu'u O'o lava lake. For a spheroidal chamber, these data imply a summit magma chamber volume of ~ 20 km^3, consistent with recent estimates from seismic tomography. Continuous deformation measurements can be used to image the spatio-temporal evolution of propagating dikes, and reveal quantitative information about the volcanic plumbing systems.

Introduction

Continuous Global Positioning System (GPS) measurements preceding the January 30, 1997 eruption on Kilauea volcano, Hawaii constrain the temporal evolution of deformation associated with dike propagation in unprecedented detail [*Owen et al.,* 2000a]. Figure 12 shows the horizontal displacements spanning the intrusion/eruption as determined from a combination of campaign and permanent GPS data. Rift extension due to dike emplacement, and contraction due to deflation of a shallow magma chamber beneath the summit of Kilauea are clearly visible in the data. Detailed analysis of the displacements indicates that, in addition to the aforementioned sources, a center of deflation was located within the East Rift Zone (ERZ) near Makaopuhi crater. The dike inferred from non-linear inversion of the surface displacements is 2.0 meters thick, aligned with the surface fissures, and dips steeply to the south [*Owen et al.,* 2000a].

The eruption began at roughly 13:00 UTC on January 30, 1997 at Napau Crater on Kilauea's East Rift Zone (Figure 12). Harmonic tremor began 8 hours prior to the eruption at 4:45 UTC, and at 5:30 UTC Kilauea's summit began to subside, indicative of melt leaving the shallow summit magma chamber. Prior to the Napau eruption magma had been erupting from the long-lived Pu'u O'o vent only a few kilometers downrift. Sometime during the early stages of the January 30'th Napau eruption, which lasted only 22 hours, magma drained from the lava pond at Pu'u O'o, leading to a two month long pause in the eruption there.

Owen et al. [2000a] showed that extension between the GPS stations NUPM and KTPM (Figure 12), began nearly coincidentally with the onset of tremor, approximately 8 hours before the eruption. NUPM, located north of the ERZ, displaced to the north, while KTPM, located south of the ERZ, displaced to the south, consistent with dike intrusion into the rift. The extension began rapidly and then slowed with time, even before the onset of the eruption [*Owen et al.,* 2000a]. We show here that the displacement time history places strong constraints on the growth of the dike prior to and during the eruption. In particular, we show that the decreasing extension rate with time is not easily explained with simple models of dike propagation at constant inlet pressure. Melt is fed to the growing dike from a number of sources, all at some distance from the dike [*Owen et al.,* 2000a]. We consider the mechanical behavior of the coupled

dike-chamber system, and show that such models predict deformation histories in reasonable accord with the observations.

Many previous theoretical studies of dike propagation have considered a constant source pressure [*Rubin,* 1993] or flux [*Lister and Kerr,* 1991] at the dike inlet [see review by *Rubin,* 1995]. These boundary conditions may be chosen more for tractability than for physical reasons. *Mériaux and Jaupart* [1998] consider a dike propagating through a plate overlying a large magma reservoir. Most recently *Ida* [1999] presented a model for dike growth including the effects of a finite sized magma chamber. Only in the case of extremely large and compressible magma reservoirs will the melt pressure at the dike inlet actually remain constant as the dike propagates. Other workers have considered the depressurization of a magma chamber in response to withdrawal of magma. *Dvorak and Okamura* [1987] showed that summit tilt changes at Kilauea followed a roughly exponential decay during subsidence events. They invoke a simple hydraulic model attributed to *Machado et al.* [1974], involving a compressible chamber connected to a magma sink by a cylindrical conduit. A central difference between *Dvorak and Okamura's* [1987] analysis and the present study is that the new GPS data constrain the deformation at the dike (the magma "sink") as well as at the Kilauea summit magma chamber (one of the magma sources).

Data

Stanford University, the Hawaiian Volcano Observatory, and the University cooperatively operate a network of permanent GPS receivers on the Big Island of Hawaii. The GPS receivers record GPS phase and pseudorange at 30 second intervals and track satellites to 5 degrees above the horizon. For the kinematic analysis, we decimated the data to an epoch interval of 5 minutes and used a 25 degree elevation mask [*Larson et. al,* 2000]. The data were processed using GIPSY/OASIS software package [*Lichten and Border*, 1987; *Zumberge et al.*, 1997], using IGS orbits and earth orientation parameters. Satellite clock offsets were estimated using the GPS receiver on Kauai (KOKB) as a reference clock. The data were used to estimate station positions, receiver clock errors, tropospheric delay parameters, and carrier phase ambiguities, which were fixed to integers where possible. We processed data from January 29th 1997 through January 31st

1997 in a continuous stretch to avoid the introduction of artificial breaks in the ambiguities or tropospheric parameters at the day boundaries. Corrections to the *a priori* estimates of the tropospheric delay at each receiver are modeled as a random walk with standard deviation of 14.7 mm per square root day, using the *Niell* [1996] mapping function.

The station coordinates were modeled as a random walk processes with a standard deviation of 30 mm $/\sqrt{\text{day}}$ = 6.1 mm $/\sqrt{\text{hr}}$ with 15 minute averaging (that is, the random walk or "process noise" is added every third epoch). Much larger values of the random walk standard deviation lead to excessive epoch to epoch scatter in the GPS positions, while considerably smaller values do not allow the full displacement to develop in the course of the transient deformation episode. *Larson et al.* [2000] compared estimates of site positions for the baseline crossing the summit caldera (UWEV-AHUP) with a nearby borehole tilt record, and suggest that a random walk standard deviation of $4.4/\sqrt{\text{hr}}$ provides good agreement between GPS and tilt. We use a slightly larger value for the January 1997 eruption due to the larger magnitude of the transient signal in this instance. Uncertainties in the kinematic position determinations were estimated from the repeatability of the station coordinates over the two weeks prior to the eruption when no transient deformation is thought to have occurred.

Figures 13 and 14 show the north and east components of displacements for stations NUPM, KTPM, and KAEP relative to station MLPM, which is located on Mauna Loa and not influenced by the intrusion. Notice that NUPM, located north of the rift, moved north during the eruption, whereas the other stations, located south of the rift, moved to the south. The data clearly show that deformation began soon after the onset of harmonic tremor, approximately 6 or 7 hours before the onset of the eruption. A striking observation is that only a fraction of the eventual displacement accumulated prior to the eruption. For example, KTPM moved south roughly 17 cm prior to the eruption, but eventually displaced nearly 30 cm by the end of day 32.

Dike Volume History

The continuous GPS measurements can be used to estimate the dike volume as a function of time, in much the same way that earthquake source time functions are estimated from seismic data. Assuming the deformation is elastic, the observed displacements are proportional to the dike volume for stations far from the dike relative to the dike depth and length. For stations closer to the dike, the displacements depend on the dike length and height, which change as a function of time as the dike is emplaced.

The measured displacement as a function of space and time is

$$u_r(\mathbf{x},t) = \int_\Sigma s_p(\boldsymbol{\xi},t) G^r_{pq}(\mathbf{x},\boldsymbol{\xi}) \mathbf{n}_q(\boldsymbol{\xi}) d\Sigma(\boldsymbol{\xi}). \quad (1)$$

In (1), $\mathbf{s}(\boldsymbol{\xi},t)$ represents the spatially and temporally varying displacement discontinuity, $p,q,r, = 1,2,3$, summation on repeated indices is implied, and $\mathbf{n}_q(\boldsymbol{\xi})$ is the unit normal to the fault surface $\Sigma(\boldsymbol{\xi})$. The $G^r_{pq}(\mathbf{x},\boldsymbol{\xi})$ are proportional to derivatives of the elastostatic Green's tensors [*e.g., Aki and Richards*, 1980]. If we restrict the dike displacement to opening ($p = 3$), and for simplicity assume that the opening is uniform on the dike surface, which is rectangular with along-strike width W and height $h(t)$, then (1) becomes

$$u_r(\mathbf{x},t) = \Delta V(t) \int_0^{h(t)} \int_0^W \frac{G^r_{3q}(\mathbf{x},\boldsymbol{\xi}) \mathbf{n}_q(\boldsymbol{\xi})}{W \cdot h(t)} d(\xi_1) d(\xi_2) \quad (2)$$

$$= \Delta V(t) F_r(\mathbf{x},t). \quad (3)$$

The kernels $F_r(\mathbf{x},t)$ were computed for stations NUPM, KTPM, and KAEP, all relative to MLPM. The volume history $\Delta V(t)$ was then found by least squares. To simplify matters we assume that the dike propagates vertically at a constant rate from an initial depth of 3 km [*Owen et al.,* 2000a]. After the eruption onset, $F_r(\mathbf{x},t)$ is constant, equivalent to a 3 km high dike just reaching the surface. We also estimate the volume change associated with a shallow magma body located beneath Makaopuhi crater.

Errors in the kinematic GPS position time series are not well understood. We estimate that the errors in the east components are roughly twice those in the north; while the vertical errors are roughly five times the north components. The detailed results are somewhat sensitive to the choice of error model, although

the qualitative pattern does not change. The estimate of $\Delta V(t)$ accounts for the fact that the GPS data were processed assuming a random walk model for the station positions. This is simply achieved by taking first differences of the data, estimating the rate of change of volume, and then integrating to obtain the volume history.

A further question is how to weight the various stations. KAEP is far from the rift zone relative to the dike height and length, and therefore insensitive to details of the dike geometry. NUPM and KTPM, on the other hand, are close to the rift and are thus somewhat sensitive to the evolving dike geometry and the presence of deflation sources within the rift zone. We have chosen to downweight NUPM and KTPM by a factor of three relative to KAEP. This leads to total volume estimates that agree well with those based on all of the campaign and continuous GPS data [*Owen, et al.,* 2000a].

Figure 15a shows the estimated volume history. The net volume at the end of day 32 is 23 million cubic meters, in good agreement with the result found by *Owen, et al.* [2000a] based on the differences in daily position estimates from the full network of GPS sites before and after the eruption. Placing more weight on the data from NUPM and KTPM increases the final volume, but does not change the shape of the curve. The predicted displacements from the inferred source time history are shown in Figures 13 and 14. Assuming a random walk error model for the station coordinates is equivalent to fitting the time derivative of the data. Thus, underestimating the rate of motion soon after the onset of tremor, as in the north component of KTPM, causes the predicted curve to be offset from the data for all subsequent times.

The most striking features of Figure 15a are the convex upward character and the fact that only two thirds of the total volume change occurred at the onset of the eruption. Figure 15b shows the volume change associated with the rift zone magma body near Makaoapuhi. The net volume decrease there is between 1.0 and 1.5 million cubic meters, again in good agreement with the 1.2 million cubic meters found by *Owen, et al.* [2000a]. Finally, Figure 15c shows the flux of magma into the dike as a function of time, obtained from a smoothed derivative of the volume history. The surprising result is that the dike moment rate, or volume flux, decreases with time after the onset of harmonic tremor. We show in the next section that simple models of dike propagation predict dike moment rates that increase with time.

Dike Propagation Under Constant Pressure

We consider the dike shown in Figure 16a, with width W, height h, and thickness δ. The dike volume is

$$V_d \cong \frac{\pi}{4}\delta h W. \tag{4}$$

For a dike subject to uniform driving pressure over the dike plane, and $h << W$, the maximum opening is given by

$$\delta \cong 2(1-\nu)\frac{\Delta p}{\mu}h \tag{5}$$

where the driving pressure is $\Delta p = p - \sigma$, with p the magma pressure in the dike, and σ the compressive stress normal to the dike plane, μ is the shear modulus, and ν is Poisson's ratio [*e.g., Pollard and Segall*, 1987]. This approximation does not account for free surface effects, which would tend to increase the opening, or the finite along strike dimension of the dike, W, which would tend to decrease the opening. From (4) and (5) the dike volume is proportional to h^2

$$V_d \cong \frac{\pi(1-\nu)}{2}\frac{\Delta p}{\mu}W h^2 \tag{6}$$

The first approximation that we might make is that the dike grows at a constant rate, and that the driving pressure remains constant. In this limit the dike volume, and hence the far-field surface displacements, are expected in increase with the square of time until the onset of the eruption. If we adopt a model in which the dike is semi-circular and grows radially (Figure 16b), then the volume will scale with the dike radius cubed and for constant propagation rate the volume would increase with time cubed until the dike intersects the surface.

The rate of dike growth, however, is controlled by the rate at which magma flows to the dike tip [*Rubin, 1995*] and is therefore not constant. The magma flow rate is proportional to the driving pressure gradient from the dike inlet to the dike tip, and the square of the aperture. Letting Δp denote the pressure at the dike inlet, the pressure gradient along the dike is proportional to $\Delta p/h$. Assuming that the width W is much greater than the opening δ, then the flow rate will be proportional to δ^2. From (5), this leads to

$$\frac{dh}{dt} \cong \frac{1}{3\eta}\left(\frac{\Delta p}{h}\right)\left(\frac{\Delta p h}{\mu}\right)^2 = \frac{\mu}{3\eta}\left(\frac{\Delta p}{\mu}\right)^3 h \tag{7}$$

where η is the magma viscosity. *Rubin* [1995] shows that this simple expression predicts the magma flow velocity to within a factor of four of that given by more complete calculations that account for variations in dike thickness and magma pressure gradient. Note that the propagation rate is proportional to dike height, so that for constant Δp dike height increases exponentially with time; $h(t) = h_0 exp(t/\tau_{prop})$ with characteristic time

$$\tau_{prop} \equiv \frac{3\eta}{\mu} \left(\frac{\mu}{\Delta p} \right)^3 . \tag{8}$$

This simple model predicts the dike height increases exponentially. Similar results are obtained for more complex models [*Mériaux and Jaupart*, 1998, Figure 15; *Ida*, 1999, Figure 3]. In the simple model here, the dike volume (proportional to h^2) grows super-exponentially until the time of the eruption; after that the volume does not change. Assuming, as discussed above, that the displacements depend to first order on the dike volume, we would predict super-exponential increase in extension across the rift prior to the eruption and no change afterward. This is clearly inconsistent with the GPS data, which show that the rate of volume change *decreased* with time and that much of the rift extension occurred after the onset of the eruption.

What is wrong with the simple model? A number of approximations are suspect. First of all the dike almost certainly does not grow at fixed along-strike width. It is reasonable to expect that the dike has a more elliptical plan shape, and may continue to propagate along strike after the dike breaches the surface. Secondly, the pressure term in the gradient driving flow, $\Delta p/h$, should be interpreted as the pressure in excess of the effective pressure in a static column of magma, $\Delta \rho g$, where $\Delta \rho$ is the difference between rock and magma density and g is the gravitational acceleration. Finally, the assumption that the dike inlet pressure remains constant is almost certainly not met [see also *Ida*, 1999]. Magma flows to the dike from one or more reservoirs and must pass through conduits of finite dimensions to reach the dike inlet. Indeed the record of tilt at Kilauea summit during the 1997 Napau eruption (Figure 17b) shows deflation of the summit magma chamber beginning soon after the onset of harmonic tremor. Notice from Figure 17b that roughly 40% of the total tilt signal during the 48 hour period shown occurred before the onset of the eruption. Figure 17 shows that the summit tilt and dike volume (from Figure 15) are mirror images,

reflecting the fact that magma leaving the summit magma chamber is intruded in the dike. It should be noted that analysis of the surface deformation shows that only a small fraction of the total magma supplied to the dike came from the shallow summit chamber [*Owen et al.,* 2000a]. Nevertheless, the strong association of summit tilt and dike volume suggests that there are other time constants, controlled by the rate at which magma flows to the dike inlet, that govern dike propagation.

Coupled magma chamber dike system

Consider the simple model of a single magma chamber connected to a propagating dike (Figure 18). The actual situation during the 1997 Napau eruption was undoubtedly more complex. We have evidence from the geodetic displacements of a second magma reservoir near Makaopuhi Crater in the East Rift zone [*Owen et al.,* 2000a]. Magma was also supplied from the lava pond at Pu'u O'o, and geochemical data indicate mixing of fresh magma with melt stored within the rift zone [*Thornber,* 1997]. Nevertheless, we start by considering a single magma chamber that we loosely associate with the shallow summit reservoir.

We take the dike to be a half-ellipsoid with half length a, half height b, and maximum opening δ (Figure 18). The volume of the dike is thus

$$V_d = \frac{\pi}{3} ab\delta. \tag{9}$$

The maximum opening at the center of an elliptical penny shaped crack is

$$\delta = \frac{2b(1-\nu)\Delta p_d}{\mu E(k)}, \tag{10}$$

where $E(k)$ is the complete elliptic integral of the second kind of modulus $k = \sqrt{1 - b^2/a^2}$, [*e.g., Mura,* 1982].

We take the growth rate in length and width to be proportional to the pressure gradient and the dike aperture squared, as in (7), so that

$$\frac{da}{dt} = \frac{1}{3\eta}\left[\frac{2b(1-\nu)\Delta p_d}{\mu E(k)}\right]^2 \left(\frac{\Delta p_d}{a}\right) \tag{11a}$$

$$\frac{db}{dt} = \frac{1}{3\eta}\left[\frac{2b(1-\nu)\Delta p_d}{\mu E(k)}\right]^2 \left(\frac{\Delta p_d}{b} - \Delta\rho g\right), \qquad \Delta p_d > \Delta\rho g b \tag{11b}$$

where $\Delta\rho$ is the effective difference between the magma and rock density. As discussed by *Rubin* [1995], the gradient driving upward magma flow is $dp/dz - \rho_m g$. Because we have defined the pressure Δp as the difference between the magma pressure and the dike normal stress, this is equivalent to $d\Delta p/dz + d\sigma/dz - \rho_m g$. We take the vertical gradient of the stress to be some fraction ϵ of the lithostatic stress, i.e. $d\sigma/dz = \epsilon\rho_r g$, where ϵ must be less than unity for the least principal stress to be horizontal. Thus, we may write the effective vertical pressure gradient as $d\Delta p/dz - \Delta\rho g$, where the effective density is $\Delta\rho = (\rho_m - \rho_r) + (1-\epsilon)\rho_r$. Note also that the second equation holds only for $\Delta p_d > \rho g b$, and $db/dt = 0$ otherwise.

Equations (11) describe one dimensional flow along each of the principal axes of the dike, and thus do not account for the radial divergence in two dimensional flow from an inlet. For pressure p_0 prescribed at an inlet of radius r_0, the fluid velocity is given by

$$v_r = \frac{p_0 \delta^2}{3\eta\ r\ log(R/r_0)} \tag{12}$$

where δ is the width of the opening, and R is the radial distance at which the pressure drops to zero. The dike propagation rate can thus be approximated by the velocity at the dike tip, which is taken at $r = R$. At this level of approximation, the dike growth rate dR/dt is identical to (11) except for the $log(R/r_0)$ term. The logarithmic term is sufficiently weak that numerical solutions are not significantly altered at early times when the dike is expected to be circular. Further work is needed to address flow into an elliptical dike.

Prior to the onset of the eruption, mass is conserved in the dike and chamber. This requires $dm_d/dt = -dm_c/dt = q$, where m_d is the mass of magma in the dike, m_c is the mass of magma in the chamber and q is the mass flux from the chamber to the dike. Assuming the magma flux is proportional to the pressure difference between the chamber and the dike, $q = -c(p_d - p_c)$, so that conservation of mass implies

$$\frac{dm_d}{dt} = -\frac{dm_c}{dt} = c(\Delta p_c - \Delta p_d) \tag{13}$$

The constant c depends on the conduit geometry and the melt viscosity. The dike geometry is sufficiently

compliant that we can ignore the compressibility of the magma, i.e., $d(m_d)/dt = \rho_m dV_d/dt$, and

$$\frac{dV_d}{dt} = \frac{c}{\rho_m}(\Delta p_c - \Delta p_d). \tag{14}$$

The magma chamber, on the other hand, may be nearly spherical, and therefore much less compliant than the dike. In this case we include the magma compressibility and write

$$\frac{dm_c}{dt} = \rho_m \left(\frac{dV_c}{dt} + V_c \beta_m \frac{d\Delta p_c}{dt} \right) \tag{15}$$

where β_m is the magma compressibility. We can also define an effective magma chamber compressibility, $\beta_c = (1/V_c)dV_c/dp_c$. For example, for a spherical magma chamber at a depth significantly greater than its radius, $\beta_c = 3/4\mu$ [*e.g., McTigue, 1987*]. With this definition of β_c (15) becomes

$$\frac{dm_c}{dt} = \rho_m V_c (\beta_m + \beta_c) \frac{d\Delta p_c}{dt}. \tag{16}$$

From this point onward, we will use $\bar{\beta_c} = (\beta_m + \beta_c)$ to indicate the compressibility of the magma chamber, including both the compressibility of the cavity and the magma.

Combining (16) and (13) yields an equation governing the magma chamber pressure

$$\frac{d\Delta p_c}{dt} = \frac{-c}{\rho_m V_c \bar{\beta_c}}(\Delta p_c - \Delta p_d). \tag{17}$$

The chamber pressure decreases when it is at higher pressure than the dike, and melt flows out of the magma chamber. For the dike we combine mass conservation (14) with the dike volume relation (9) and (10) to find

$$\frac{d\Delta p_d}{dt} = \frac{3\mu c E(k)}{2\pi(1-\nu)\rho_m} \frac{(\Delta p_c - \Delta p_d)}{ab^2} - (1-A)\frac{\Delta p_d}{a}\frac{da}{dt} - (2+A)\frac{\Delta p_d}{b}\frac{db}{dt}, \tag{18}$$

where A is defined as

$$A = \left(\frac{E-F}{E}\right)\left(\frac{1}{a^2/b^2 - 1}\right). \tag{19}$$

In deriving (18) we have made use of the fact that $dE/dk = (E-F)/k$, where F is the complete elliptic integral of the first kind with modulus k. The first term on the right hand side of (18) represents flow of magma from the chamber into the dike. Flow acts to increase the magma pressure in the dike whenever the

chamber pressure exceeds that in the dike. The remaining two terms are related to dike growth. If there is no flow into the dike ($c = 0$), then the mass of melt in the dike remains constant and the magma pressure must decrease as the dike propagates. The quantity A ranges from zero for a thin blade like dike to -0.5 for a circular crack, so that the second and third terms on the right hand side of (18) are never positive when the dike is growing ($da/dt > 0, db/dt > 0$).

Equations (17) and (18) together with the dike propagation equations (11) form a system of 4 coupled non-linear equations in the variables ($\Delta p_c, \Delta p_d, a$, and b).

The above results hold only when mass is conserved in the dike-chamber system. Once the dike breaches the surface and begins to erupt, equation (14) is no longer valid. At this point the mass change within the dike is the difference between the flux into the dike, q, and the flux to the surface. We take the latter to be proportional to the difference between the pressure at the dike inlet and the magma static pressure. Thus, (14) is replaced with

$$\frac{dV_d}{dt} = \frac{c}{\rho_m}(\Delta p_c - \Delta p_d) - \frac{c_2}{\rho_m}(\Delta p_d - \Delta\rho g d), \tag{20}$$

where the constant c_2 depends on the dimensions of the dike and the magma viscosity, and d is the dike height (equal to the depth, since the dike reaches the surface). Combining (20) with the dike volume relation (9) and (10), yields an expression for the pressure change within the dike

$$\frac{d\Delta p_d}{dt} = \frac{3\mu E(k)}{2\pi(1-\nu)d^2 a}\left[\frac{c}{\rho_m}(\Delta p_c - \Delta p_d) - \frac{c_2}{\rho_m}(\Delta p_d - \Delta\rho g d)\right] - (1-A)\frac{\Delta p_d}{a}\frac{da}{dt}. \tag{21}$$

The first term in the square brackets represents flow into the dike, the second eruptive flow onto the earth's surface. The final term represents a pressure decrease due to continued along strike propagation. We can approximate the flux out of the dike by assuming flow through a tabular conduit of height d, thickness δ, and along strike length ωa, where $0 < \omega < 2$. That is, the length of the eruptive fissure is approximated as some fraction of the dike length, $2a$. In this case $c_2 = \rho_m \delta^3 \omega a / 12\eta d$ [e.g., *Bird, et al.*, 1960], and δ is given by (10). This is a crude approximation that may be good for short times following the onset of the eruption. As time progresses, magma within the dike begins to freeze, channeling flow to a single circular vent, which can more efficiently transport magma to the surface [*Delaney and Pollard*, 1981]. This process

occurs on a time scale of a few days. We leave thermal effects for future analysis, and note that in the isothermal limit the volume flux out of the dike (second term in equation (21)) is

$$q_{erupt} = \frac{2(1-\nu)^3 d^2 \omega a \Delta p_d^3}{3\eta\mu^3 E^3(k)}(\Delta p_d - \Delta\rho g d) \qquad \Delta p_d > \Delta\rho g d. \tag{22}$$

The flux in (22) can be integrated to yield the total erupted volume. With this approximation for c_2 and the dike opening given by (10), equation (21) becomes

$$\frac{d\Delta p_d}{dt} = \frac{3\mu c E(k)}{2\pi(1-\nu)\rho_m a d^2}(\Delta p_c - \Delta p_d) - \frac{\mu(1-\nu)^2\omega}{\pi\eta E^2(k)}\left(\frac{\Delta p_d}{\mu}\right)^3(\Delta p_d - \Delta\rho g d) - (1-A)\frac{\Delta p_d}{a}\frac{da}{dt}. \tag{23}$$

Note again, that the first term represents pressure change due to flow into the dike from the magma chamber, the second pressure loss due to eruptive flux out of the dike, and the third pressure loss due to lateral propagation of the dike. We assume that the second term holds only for $\Delta p_d \geq \Delta\rho g d$, although one could imagine drainback occurring if the pressure dropped below $\Delta\rho g d$.

We can further approximate the eruptive length ωa by imagining that the dike continues to grow with height according to (11b) even above the earth's surface (Figure 19). The intersection of the fictitious ellipse with the free surface, *i.e.,* $\omega = 2\Re(\sqrt{1 - d^2/b^2})$, where $\Re$ indicates real part, provides a measure of the along strike fissure dimension ωa. This measure of eruptive length scales with the total dike length, and allows ω to increase if the dike has sufficient pressure such that b would have exceeded the depth d.

Non-dimensionalization

We normalize the pressures Δp_c and Δp_d by the initial pressure Δp_0, assumed equal in the dike and chamber, as no flow occurs in the initial state. The dike height is normalized by the depth d, and time by the characteristic time for magma propagation, τ_{prop}, where τ_{prop} is defined, as in (8), at the initial pressure Δp_0,

$$\tilde{p}_c = \frac{\Delta p_c}{\Delta p_0}; \quad \tilde{p}_d = \frac{\Delta p_d}{\Delta p_0}; \quad \tilde{a} = \frac{a}{d}; \quad \tilde{b} = \frac{b}{d}; \quad \tilde{t} = \frac{t}{\tau_{prop}}; \tag{24}$$

where

$$\tau_{prop} = \frac{3\eta}{4(1-\nu)^2\mu}\left(\frac{\mu}{\Delta p_0}\right)^3. \tag{25}$$

This leads to the following system of equations:

$$\frac{d\tilde{a}}{d\tilde{t}} = \frac{\tilde{p}_d^3\tilde{b}}{E^2(k)}(\tilde{b}/\tilde{a}) \tag{26a}$$

$$\frac{d\tilde{b}}{d\tilde{t}} = \begin{cases} \frac{\tilde{p}_d^2\tilde{b}}{E^2(k)}(\tilde{p}_d - \alpha\tilde{b}) & \text{if } \tilde{b} < 1 \text{ and } \tilde{p}_d > \alpha\tilde{b} \\ 0 & \text{otherwise} \end{cases} \tag{26b}$$

$$\frac{d\tilde{p}_d}{d\tilde{t}} = \begin{cases} \mathcal{R}\frac{E(k)}{\tilde{a}\tilde{b}^2}(\tilde{p}_c - \tilde{p}_d) - (1-A)\frac{\tilde{p}_d}{\tilde{a}}\frac{d\tilde{a}}{d\tilde{t}} - (2+A)\frac{\tilde{p}_d}{\tilde{b}}\frac{d\tilde{b}}{d\tilde{t}} & \text{if } \tilde{b} < 1 \\ \mathcal{R}\frac{E(k)}{\tilde{a}}(\tilde{p}_c - \tilde{p}_d) - (1-A)\frac{\tilde{p}_d}{\tilde{a}}\frac{d\tilde{a}}{d\tilde{t}} - \frac{3\omega}{4\pi E^2(k)}\tilde{p}_d^3(\tilde{p}_d - \alpha) & \text{if } \tilde{b} = 1 \end{cases} \tag{26c}$$

$$\frac{d\tilde{p}_c}{d\tilde{t}} = -\mathcal{R}\Psi(\tilde{p}_c - \tilde{p}_d) \tag{26d}$$

where the three non-dimensional quantities are

$$\alpha = \frac{\Delta\rho g d}{\Delta p_0} \tag{27a}$$

$$\mathcal{R} = \frac{\tau_{prop}}{\tau_{flow}} = \frac{9\eta c\mu^3}{8\pi\rho_m((1-\nu)\Delta p_0 d)^3}; \qquad \tau_{flow} = \frac{2\pi(1-\nu)\rho_m d^3}{3\mu c} \tag{27b}$$

$$\Psi = \frac{2\pi(1-\nu)d^3}{3V_c\bar{\beta}_c\mu} \tag{27c}$$

and τ_{flow} is the characteristic time for flow between the magma reservoir and a stationary dike with height $\tilde{b} = 1$ and length $\tilde{a} = 1$.

The first two of the governing equations are just the non-dimensional form of (11), and control the rate of horizontal and vertical dike propagation, respectively. We find, as before, that the rate of dike propagation is proportional to dike length and to the cube of the dike driving pressure. Propagation in the vertical is controlled by the pressure in excess of the effective magma-static gradient, $\alpha\tilde{b}$. The dimensionless parameter α is the ratio of the pressure due to a static column of magma with depth d to the initial dike pressure. When $\alpha << 1$ the weight of the overlying magma provides very little resistance to upward flow. On the other hand if α is only slightly less than unity, there is little overpressure to drive vertical flow.

The third equation in (26) shows that the rate of change of dike pressure is governed by the rate of dike growth (second and third terms on right hand side), which causes the pressure to decrease, and influx from

the magma reservoir (first term on right hand side), which causes the pressure to increase. The relative rates of these processes is controlled by the non-dimensional quantity $\mathcal{R}$ which is the ratio of the characteristic time for dike propagation to that for magma flow into the dike. When $\mathcal{R}$ is large the rate of flow to the dike is fast and the dike propagates at nearly constant pressure. When $\mathcal{R}$ is small flow into the dike is slow, and propagation may be limited by magma supply. The fourth equation governs the pressure history in the magma chamber, and depends on the product of the dimensionless quantities $\mathcal{R}$ and Ψ. The latter can be put in a more interpretable form, by noting that the compressibility of the dike $\beta_d = (1/V_d)dV_d/dp_d$ can be computed from equations (9) and (10). This allows one to write Ψ as

$$\Psi = \frac{\pi V_d^f \beta_d}{2V_c \bar{\beta}_c} \tag{28}$$

where V_d^f is the final volume of a semi-circular dike with radius equal to the depth d, ($a = b = d$). We have also made use of the fact that $E(k = 0) = \pi/2$. The parameter Ψ controls the chamber pressure history. If the chamber volume and/or compressibility is large compared to the dike volume and/or compressibility, $\Psi << 1$, then the chamber exhibits little pressure loss. Effectively the dike sees an infinite reservoir which supplies magma at constant pressure. At the other extreme $\Psi \geq 1$ the pressure in the magma chamber drops rapidly, which will stabilize dike growth.

Finally, we define a reference dike volume as $2\pi(1-\nu)\Delta p_0 d^3/3\mu$, so that the non-dimensional dike volume is $\tilde{V}_d = \tilde{a}\tilde{b}^2\tilde{p}_d/E(k)$. With these definitions, the non-dimensional eruptive flux is

$$\tilde{q}_{erupt} = \frac{3\omega\tilde{a}}{4\pi E(k)^3}\tilde{p}_d^3(\tilde{p}_d - \alpha) \tag{29}$$

where ω, here and in (26c) is given by $\omega = \Re(\sqrt{\tilde{b}^2 - 1})/\tilde{b}$. The flux is integrated with respect to time to give the total erupted volume.

Parameter Values

Before proceeding with numerical solution to the governing equations (26), we discuss the values of the dimensionless parameters defined in (27). The parameter α reflects the ratio of the magmastatic head to the initial dike pressure. It is useful to consider the initial magma pressure in terms of the static head of a

column of melt, e.g. $p_0 = \rho_m g(d+h)$, where d is the depth of the dike and h is the overpressure in terms of head. Δp_0 is thus $\Delta p_0 = \rho_m g(d+h) - \epsilon\rho_r g d$, and the dimensionless ratio α

$$\alpha = \left[1 + \frac{(h/d)\rho_m}{\rho_m - \epsilon\rho_r}\right]^{-1} \tag{30}$$

If ϵ, which is generally bounded by $0 \leq \epsilon \leq 1$, is too small we would anticipate normal faulting in the rift zone. While dike intrusions do trigger normal events the rift generally fails in extension rather than by faulting. According to simple frictional faulting considerations then, neglecting cohesion, $\epsilon \geq [\sqrt{f^2+1} - f]/[\sqrt{f^2+1} + f]$, where f is the coefficient of friction. For $f \sim 0.6$, ϵ must exceed 0.32. The overpressure h is unlikely to exceed a few tens of meters. For ϵ in the range $0.32 \leq \epsilon \leq 1$, $\rho_m = 2.6 \times 10^3 kg/m^3$, and $\rho_r = 2.3 \times 10^3 kg/m^3$, $0.95 \leq \alpha \leq 1$ for $h = 15$ meters, and $0.90 \leq \alpha \leq 1$ for $h = 30$ meters.

The dimensionless parameter $\mathcal{R}$ can be estimated if we define the geometry of the conduit connecting the magma chamber and the dike, which constrains the constant c in equation (13). For steady uniform flow in a circular conduit of radius r and length L,

$$c = \frac{\pi\rho r^4}{8\eta L} \tag{31}$$

[*Bird, et al.*, 1960]. Combining (31) with (27) and (10), leads to

$$\mathcal{R} \cong \frac{r^4}{\delta^3 L}. \tag{32}$$

While the average dike opening $\delta \sim 2$ meters is relatively well constrained by the GPS data, the conduit radius and length are parameters we would like to be able to constrain by the observations. For a 10 km long conduit connecting the summit magma chamber to Napau Crater with radius of 2 meters, $\mathcal{R} \sim 10^{-4}$. At the other extreme, a conduit with radius 10 m connecting Pu'u O'o and Napau Crater, with $L = 3$ km, $\mathcal{R} \sim 0.4$

The dimensionless parameter Ψ depends on the total volume and compressibility of the magma chamber feeding the dike, again parameters we would like to estimate from the data. Measurements of surface displacements, tilts, or strains give the *change* in volume of the magma chamber. For a spherical chamber,

the displacements are also related to the product of the change in chamber pressure and the radius cubed $p_c a^3$, where p_c is understood to be the change in pressure accompanying deformation, and a is the chamber radius [*McTigue,* 1987]. Independent constraints on the change in magma pressure allow one to estimate the chamber volume. It has been observed that changes in the level of magma in a lava pond correspond to changes in tilt measured at Kilauea summit [*Tilling,* 1987], suggesting that the lake levels may be used as a manometer to measure magma pressure [*e.g., Denlinger,* 1997]. Lava lake levels may change due to other processes, including changes in density due to degassing (so called "gas-piston" activity), however large changes in lava level probably reflect changes in pressure within the magmatic system.

Denlinger [1997] noted that during a period of declining magma efflux the summit tilt varied quadratically, changing from deflation to inflation. This observation allowed him to to relate the summit tilt to changes in magma volume. He also used changes in lava level to relate summit tilt changes to magma pressure. With these data he estimated the total volume of Kilauea's magma system to be 240 km^3 (160 km^3 to 320 km^3).

The long pause in the eruption at Pu'u O'o following the January 30, 1997 eruption can be used to place constraints on the size of the summit magma chamber. Lava was first sighted in the Pu'u O'o pond on February 24, 1997 [*Harris et al.,* 1997]. At this point the lava level was 250 ± 10 meters beneath the north rim of the cone [*Thornber,* personal communication, 1999]. By March 21, 1997 the depth of the lava lake had increased by ~ 100 meters (150 meters beneath the north rim). Thus, between February 24 and March 21, the lake level rose 100m, corresponding to a pressure increase of 2.7 Mpa.

During this same time, the GPS baseline AHUP-UWEV continuously extended, indicating an increase in the volume of the summit magma chamber (Figure 20). The GPS data can be used to estimate the change in the volume of the magma chamber, assuming a spherical source beneath Kilauea summit. While *Owen et al.* [2000a] found a source depth of 1 to 2 km for the deflation associated with the 1997 Napau eruption, *Dvorak and Okamura,* [1987] estimate chamber depths of 3 to 5 km from analysis of tilt data. *Owen et al.* [2000b] estimate the depth of a deflating chamber at between 0.5 to 3.5 km from campaign GPS measurements between 1990 and 1996. In this analysis we assume a source depth of 3 km.

We used the daily GPS position determinations and covariance matrices to estimate the rate of volume

change, assuming a constant rate during the one month interval. The fit to the horizontal components of the GPS baseline are shown in Figure 20. The computed volume change is 2.3×10^{-3} km^3, leading to $dV/dP = 0.8m^3/Pa$, much smaller than estimated by *Denlinger* [1997], but similar to the $0.6m^3/Pa$ value estimated by *Johnson* [1992] for the refilling of the Mauna Ulu lava lake in May of 1973.

The volume of the magma chamber is then given by

$$V_c = \beta_c^{-1}(1 - p_c\beta_m)\frac{dV_c}{dp*_c}, \tag{33}$$

where β_c is the magma chamber compressibility defined after equation (15), $dp*_c$ is the apparent pressure change, i.e., that given by $\rho_m g dh$, dh being the change in height of the magma pond. For a spherical magma chamber, $\beta_c^{-1} = 4\mu/3$. For a shear modulus μ of 20 GPa and magma compressibility β_m of 0.1 GPa^{-1} [*Fujii and Kushiro,* 1977], we estimate V_c to be ~ 20 km^3, which agrees rather well with estimates of 27 km^3 from seismic tomography [*Dawson et. al.,* 1999]. A volume of 20 km^3 corresponds to a magma chamber radius of 1.7 km, only half the source depth. *McTigue* [1987] however, showed that the effects of chamber finiteness are small even for radius to depth ratios of 0.5.

Our estimate of the summit magma chamber volume is substantially less than the 240 km^3 that *Denlinger* [1997] estimates for Kilauea's magma system, including both summit and rift magma reservoirs. *Denlinger's* [1997] estimate may be biased if magam intrudes the deep rift zone, as suggested by the work of *Delaney et al.* [1990] and *Owen et al.* [1995], at a rate that varied with time. Our estimate could be biased if the magma chamber geometry departs significantly from an equant chamber. Taking the full range of estimated V_c, Ψ lies in the range 0.03 to 0.4.

Modeling of the deformation accompanying the Napau eruption demonstrated that only a fraction of the magma supplied to the dike and the eruption came from the summit chamber [*Owen, et al.* 2000a]. It is estimated that $\sim 10^6 m^3$ of lava drained from Pu'u O'o during the Napau eruption, approximately half of the magma supplied to the dike and eruption [*Hawaii Volcano Observatory, unpublished data*]. Including a surface lava pond as a magma supply requires only modest modification to the coupled chamber dike equations.

Write equation (15), ignoring the effects of melt compressibility as

$$\frac{dm_c}{dt} = \rho \frac{dV_c}{dp_c} \frac{dp_c}{dt} \tag{34}$$

Assuming we can model the lava pond as a cylinder of radius r_p, and noting that the pressure at the base of the cylinder is ρg times the height of the magma column, $V_c = \pi r_p^2 p_c / \rho g$. Combining this with (34) and (13) leads to

$$\frac{dp_c}{dt} = \frac{-cg}{\pi r_p^2}(p_c - p_d) \tag{35}$$

which is of precisely the same form as (17). Thus, the governing equations do not change as long as we interpret Ψ to be

$$\Psi = \frac{2(1-\nu)\rho_m g d^3}{3\mu r_p^2}. \tag{36}$$

For a radius r_p of 100 m, and the range of shear moduli discussed above, Ψ ranges from order 1 to 10.

Solutions to the Coupled Equations

Analytical solutions to the governing equations are difficult to find. The results of *Dvorak and Okamura,* [1987], are recovered from equation (17) if we assume that the dike pressure p_d suddenly drops to a constant value $p_d < p_c$. This leads to a chamber pressure that decays exponentially with time constant

$$\tau_{chamber} = \frac{8\eta V_c \beta_c L}{\pi r^4}, \tag{37}$$

assuming a cylindrical conduit with radius r and length L. *Dvorak and Okamura* [1987] discuss evidence that subsidence events associated with lower East Rift Zone eruptions (large L) are associated with longer summit tilt events. More generally, the duration of the summit tilt excursion depends on both the hydraulic properties of the system and how rapidly the dike propagates and the pressure drops.

In the limiting case that the dike inlet pressure does not change with time, and the aspect ratio $b/a << 1$, so that $E(k) \cong 1$, then (26b) is simply integrated to yield

$$\tilde{b}(\tilde{t}) = \frac{\tilde{b}_0 e^{\tilde{t}}}{\alpha \tilde{b}_0 (e^{\tilde{t}} - 1) + 1}. \tag{38}$$

At short dimensionless times the dike growth is exponential, as expected from earlier discussion, however at longer times the dike height approaches a constant equal to $1/\alpha$. If the initial magma pressure is not much over magma-static, that is α is close to 1, the dike will slow as it approaches the surface. If $\alpha = 1$ the dike does not reach the surface in finite time. This effect is likely to be important in explaining the observed source time history. Coupling between the dike and magma reservoirs must also be important, since measured tilt and GPS displacements confirm pressure declines within these magma bodies at the same time the dike was being emplaced.

The non-dimensional first-order non-linear ordinary differential equations were integrated numerically with initial conditions: $\tilde{p}_d(0) = \tilde{p}_c(0) = 0$, and $\tilde{a}(0) = 2\tilde{b}(0) = 0.02$. The initial pressure in the dike and the magma chamber are identical and equal to the dike normal stress. The dike is initially slightly elongate along strike, however the dimensions are only 2% of the depth beneath the Earth's surface. Solutions are stopped after either some nominal time is exceeded, the difference between the dike and magma chamber pressures falls below a critical value, or the dike length along strike exceeds some value.

Example solutions, not necessarily intended to fit the data from the Napau 1997 eruption, are shown in Figure 21. The first few examples consider large values of $\mathcal{R}$ so that the characteristic time for flow between the chamber and dike is small, and the dike and chamber pressures remain nearly equal. The result for $\mathcal{R} = 20, \Psi = 0.01, \alpha = 0.95$ is shown with a solid line. The dike height increases rapidly until the dike hits the surface $\tilde{b} = 1$. As the dike is propagating upward the aspect ratio, which is initially elongate along strike, becomes more circular and $\tilde{a}/\tilde{b} \sim 1$. This is due to the fact that if one dimension becomes shorter than the other, the pressure gradient in that direction increases and the dike speeds up. Thus, for small dikes the tendency is for circular plan shapes. This holds until the dike begins to sense the gravitational resistance to upward flow. From this point onward the dike grows far more readily in the horizontal direction than the vertical, leading to an elongate blade-like intrusion [see also *Rubin*, 1995]. The model predicts a small amount of erupted material, but less than 1% of the intruded volume. At the end of the run the dike and chamber pressures are nearly equal. While we do not model thermal effects, it is safe to consider that without a pressure difference to drive flow the dike is "frozen".

Modifying any of the parameters significantly alters the predicted behavior. Increasing α even slightly to 0.97 results in an intrusion rather than eruption (Figure 21). This come about by slightly decreasing the initial pressure Δp_0 or by decreasing the dike normal stress by decreasing ϵ. For example, with an overpressure of h of 15 meters, $\rho_m = 2.6 \times 10^3 kg/m^3$, and $\rho_r = 2.3 \times 10^3 kg/m^3$, and $\epsilon = 1$, α is approximately 0.95. Decreasing ϵ slightly to 0.91 increases α to 0.97. In this particular example the dike gets extremely close to the surface, $\tilde{b} = 0.99$, so that one could imagine that vesiculation could buffer the pressure near the dike tip, permitting an eruption. Nevertheless, the important result is that low initial pressures and/or extensional stress environments favor intrusion rather than eruption. In this example the dike continues to propagate horizontally for a long time before the run is terminated. In actual rift zones the dike normal principal stress presumably varies due to a number of processes including previous intrusion events. It is reasonable to imagine that the dike stops propagating if it runs into a region of sufficiently low driving stress, $\Delta p = p - \sigma$.

Increasing Ψ also decreases the tendency for the dike to reach the surface and initiate an eruption. The effect of increasing Ψ to 0.1 is shown as the dashed line in Figure 21. With a smaller or less compressible magma chamber the pressure drops more dramatically stabilizing the dike. In this example the dike height reaches $\tilde{b} = 0.91$, and length $\tilde{a} \cong 15$. At this point the pressure difference between the chamber and the dike is 10^{-4} of the initial pressure and the dike is frozen. Note again the tendency to produce elongate, blade-like dikes.

Finally, we consider the effect of varying $\mathcal{R}$, the ratio of characteristic times for dike propagation (at constant driving pressure) and flow between the magma chamber and the dike. Figure 21 illustrates the effect of decreasing $\mathcal{R}$ to 0.1. Because flow into the dike is restricted, the dike pressure drops much more dramatically than for large values of $\mathcal{R}$, stabilizing the dike. Note that the dike pressure actually begins to rise after the dike stops propagating vertically. With $\Psi = 0.01$, the magma source is sufficiently large that the dike continues to grow along strike until the computation is stopped.

All three parameters thus effect the tendency for a dike to reach the surface initiating an eruption. Small values of α corresponding to high initial magma pressures and/or relatively large dike normal compression

(although the dike normal stress must be the minimum principal stress) favor eruptions. Decreasing the initial dike pressure or the dike normal compression favors intrusion. Small Ψ corresponding to large compressible magma reservoirs favor eruption. With larger values of Ψ the magma pressure drops favoring intrusion. Finally the hydraulics of the plumbing system connecting the dike and chamber, through parameter $\mathcal{R}$ effect the duration of the process and the tendency for eruption. For small values of $\mathcal{R}$ flow into the dike is slow and the dike pressure drops, stabilizing the dike and inhibiting eruptions. Large values of $\mathcal{R}$ corresponding to highly conductive conduits favor eruptions.

Comparison to Data

A goal of this work is to use observations to constrain the physical properties of the volcanic system. We can compare these models to the dike volume history (Figure 17a), which has been directly estimated from the GPS observations. The summit tilt record (Figure 17b) reflects the temporal evolution of the magma chamber pressure. In addition, inversion of the GPS data showed that the final dike length is roughly twice the depth [*Owen et al.,* 2000a]. Geologic and geodetic observations constrain the relative volumes of erupted and intruded basalt [*Owen et al.,* 2000a].

We searched a subspace of the $\mathcal{R}, \Psi, \alpha$ parameter space to determine: i) whether the dike is predicted to reach the surface, ii) the ratio of the dike volume at the onset of the eruption to the final dike volume, iii) the ratio of erupted to intruded volume, iv) the ratio of the magma chamber pressure at the onset of the eruption to the final chamber pressure. In none of the cases we examined were we able to fit all of the observations, indicating that the simple description is lacking in some significant aspects.

The solution for $\mathcal{R} = 20, \Psi = 0.01, \alpha = 0.95$ in some way mimics the observations, in that the erupted volume is very small compared to the intruded volume, and the dike volume at the onset of the eruption is a small fraction of the final dike volume. There are two problems with models of this sort, however. First, $\mathcal{R}$ of 20 is substantially larger then we judge to be reasonable, and would require a very wide short conduit connecting the magma reservoir and dike. Secondly, the dike aspect ratio b/a becomes very small as the dike continues to propagate until the reservoir pressure is depleted. As discussed above, lateral variations

in the magnitude of the dike normal stress may limit the dike length.

We examined solutions in which along-strike dike propagation is artificially terminated when the length equals twice the dike depth. Figure 22 shows representative results. In this case, the magma pressure within the dike begins to recover after the dike stops propagating downrift. The dike never reaches the surface, however. It should be noted that calculations ignore the effects of vesiculation which will act to buffer the pressure near the dike tip. As this effect becomes important in the upper few hundred meters for basalts [*Wilson and Head,* 1981], vesiculation will tend to influence dikes that would otherwise stall very close to the surface. Including the effect of vesiculation could allow dikes such as those in Figure 22 to breach the surface. On the other hand, cooling of the melt during intrusion results in large changes in apparent viscosity and ultimately freezing of the basalt. Thermal effects likely limit dike propagation at low velocities and are central in how flow develops during the course of an eruption [*Delaney,* 1982].

It should also not be forgotten that the single magma chamber model considered here is probably not appropriate to the 1997 Napau eruption on Kilauea. We have good evidence that magma was supplied to the dike not only from the summit magma chamber, but also the lava pond at Pu'u O'o, and quite likely from magma reservoirs within the East Rift Zone [*Owen et al.,* 2000a]. Given the small size of the 1997 dike, the distribution of measurements, and our lack of knowledge of the time history of magma leaving the Pu'u O'o lava pond, it is not feasible to explore multi-chamber models. Finally, the lumped parameter description, which does not allow for spatial variability in any of the field parameters, such as dike pressure, is likely to be limited in its ability to make quantitative predictions.

However, it should be possible with improved spatial coverage of surface displacement, strain, and tilt, to far better constrain the spatio-temporal evolution of dikes as they are emplaced, particularly for larger dikes for which the signal to noise ratio will be higher. In these cases it will be possible to invert for dike growth history, both horizontally and vertically, as well as the dike volume as a function of time. Comparing these observations with models of the type developed here should allow us to infer much about the plumbing system of volcanoes, including the size and shape of magma reservoirs, and the effective dimensions of conduits that supply magma to the growing dike. Ultimately, it may prove possible to use the time history

of deformation measured at the Earth's surface to predict whether a growing dike will end in an eruption or an intrusion.

Conclusions

Continuous measurements of deformation accompanying dike intrusions can be used to determine the dike volume history, effectively the source time function of the dike. The volume history can be used to place constraints on the dynamics of dike propagation. For the 1997 Napau eruption at Kilauea, we find the dike volume-rate decreased with time and that only two thirds of the dike volume accumulated prior to the onset of the eruption. At present it is unknown whether these are common characteristics of basaltic dike intrusions.

The summit magma chamber's deflationary tilt history closely mirrors the volume increase in the dike, strongly suggesting that the two magma bodies are coupled, and the dike pressure decreased during propagation. For a simple lumped parameter model of the coupled dike magma-chamber system the predicted behavior depends on three dimensionless parameters: $\mathcal{R}$, the ratio of the characteristic time for dike propagation to the characteristic time for magma flow between the chamber and the dike; Ψ measures the compressibility and size of the magma chamber relative to the dike; and α, the ratio of the effective head of a column of melt equal to the depth of the dike to the initial pressure within the dike. Whether or not the dike breaches the surface, leading to an eruption, depends on these dimensionless parameters. Eruptions are favored by small α, equivalent to large initial pressures and/or relatively compressive stress normal to the dike, small Ψ equivalent to large magma chambers, and large $\mathcal{R}$ corresponding to high hydraulic conductivity between the chamber and the dike.

Model predictions are compared to the ratio of the dike volume at the onset of the eruption to the final dike volume, the ratio of erupted to intruded volume, the ratio of the magma chamber pressure at the onset of the eruption to the final chamber pressure. While we were unable to fit all of the observations satisfactorily, the best fits were obtained for values of $\mathcal{R}$ considerably larger than expected. This may suggest that much of the magma filling the dike came from nearby sources through highly conductive

sources. Similarly, *Owen et. al.,* [2000a] found that only a small fraction of the melt was supplied directly from the shallow summit magma reservoir. At the same time interpretation is complicated by the likelihood that the dike was fed from multiple sources, including magma chambers at Kilauea summit, and the East Rift Zone, as well as the lava lake at Pu'u O'o. In addition, magma vesiculation, thermal effects, and variations in dike-normal stress complicate quantitative analysis. More observations are needed to see if other dikes grow in a similar fashion to the 1997 Napau dike, and to determine whether the simple model of coupled dike and magma chambers has useful predictive capabilities.

Acknowledgments. We thank Allan Rubin for insightful and important discussions that materially influenced the progress of this study, and Norm Sleep for valuable discussions. Reviewers, R. Denlinger and Y. Okada and Associate Editor Allan Rubin provided helpful comments. The NSF and USGS have funded our work on Kilauea.

References

Aki, K. and P.G. Richards, *Quantitative Seismology: Theory and Methods*, 932 pp., W. H. Freeman, New York, 1980.

Bird, R.B., W.E. Stewart, and E.N. Lightfoot, *Transport Phenomena*, John Wiley and Sons, New York, 780, p., 1960.

Dawson, P.B., B.A. Chouet, P.G. Okubo, A. Villesanor, and H.M. Benz, Three dimensional velocity structure of the Kilauea caldera, Hawaii, *Geophys. Res. Letters,* v 26, 2805-2808, 1999.

Delaney, P. T., R. S. Fiske, A. Miklius, A. T. Okamura, M. K. Sako, Deep magma body beneath the summit and rift zones of Kilauea Volcano, Hawaii *Science 247*, 1311, 1990.

Delaney, P. T. and D. D. Pollard, Deformation of host rocks and flow of magma during grow of minette dikes and brecia-bearing intrusions near ship rock, New Mexico, *U.S.G.S. Professional Paper 1202,* 1981.

Delaney, P.T. Solidification of basaltic magma during flow in a dike, *Amer. Jour. Sci* 282, 856-885, 1982.

Denlinger, R.P., A dynamic balance between magma supply and eruption rate at Kilauea volcano, Hawaii, *Jour. Geophys. Res.* v. 102, 18,091-18,100, 1997.

Dvorak, J.J. and A. T. Okamura, A hydraulic model to explain variations in summit tilt rate at Kilauea and Mauna Loa volcanoes, in *Volcanism in Hawaii*, U.S. Geological Survey Prof. Paper, 1350, edited by R.W. Decker, T.L. Wright, and P. H. Stauffer, 1987.

Fujii, T. and I. Kushiro, Density, viscosity, and compressibility of basaltic liquid at high pressures, in *Annual Report of the Director 1976-1977* Geophysical Laboratory, pp. 419-424, Carnegie Institute of Washingtion, D.C., 1977.

Johnson, D. J., Dynamics of magma storage in the summit reservoir of Kilauea volcano, Hawaii, *Jour. Geophys. Res.* v 97, 1,807-1,820, 1992.

Harris, J.L., L. Keszthelyi, L.P. Flynn, P.J. Mouginis-Mark, C. Thornber, J. Kauahikaua, D. Sherrod, F. Trusdell, M.W. Sawyer and P. Flament, Chronology of the episode 54 eruption at Kilauea volcano, Hawaii, from GOES-9 satellite data, *Geophysical Research Letters,* 24, p.3281-3284, 1997.

Ida, Y., Effects of crustal stress on the growth of dikes: conditions of intrusion and extrusion of magma, *Jour. Geophys. Res.* v 104, 17, 897- 17, 909, 1999.

Larson, K.M., P. Cervelli, M. Lisowski, A. Miklius, P. Segall, and S. Owen, Volcano monitoring using kinematic GPS: Filtering strategies, *Jour. Geophys. Res.*, in revision, 2000.

Lichten, S.M. and J.S. Border, Strategies for high-precision global positioning system orbit determination, *Jour. Geophys. Res.*, Vol. 92, no. 12, p. 12,751-12,762, 1987.

Lister, J. R. and R.C Kerr, Fluid mechanical models of crack propagation and their application to magma transport in dykes, *Jour. Geophys. Res.* v. 96, 10,049-10,077, 1991.

Machado, F., The search for magmatic reservoirs, in *Physical Volcanology*, Developments in solid earth geophysics, v. 6, edited by L. Civetta, P. Gasparinit, G. Luongo, and A. Rapolla, p. 255-273, Elsevier, Amsterdam, 1974.

McTigue, D.F., Elastic stress and deformation near a finite spherical magma body: resolution of the point source paradox, *Jour. Geophys. Res.*, v. 92, 12,931-12,940, 1987.

Mériaux, C. and C. Jaupart, Dike propagation through and elastic plate, *Jour. Geophys. Res.*, v. 103, 18,295-18,314, 1998.

Mura, Toshio, Micromechanics of defects in solids, M. Nijhoff, The Hague, 494 p, 1982.

Niell, A.E., Global mapping functions for the atmposphere delay at radio wavelengths, *Jour. Geophys. Res.*, v. 101, 3227-3246, 1996.

Owen, S., P. Segall, J. Freymueller, A. Miklius, R. Denlinger, T. Arnadottir, M. Sako, and R. Burgmann, Rapid deformation of the south flank of Kilauea volcano, Hawaii,*Science,* v 267, p. 1328-1332, 1995.

Owen, S., P. Segall, M. Lisowski, M. Murray, M. Bevis, and J. Foster, The January 30, 1997 eruptive event on Kilauea Volcano, Hawaii, as monitored by continuous GPS, *Geophysical Research Letters*, v. 27, 2757-2760, 2000a.

Owen, S., P. Segall, M. Lisowski, A. Miklius, R. Denlinger, M. Sako, The rapid deformation of Kilauea volcano: GPS measurements between 1990 and 1996, *J. Geophys. Res.,* v.105, 18,983-18,998, 2000b.

Pollard, D.D., and P. Segall, Theoretical displacements and stresses near fractures in rock: with application to faults, joints, veins, dikes, and solution surfaces, In *Fracture Mechanics of Rock*, Academic Press, p. 227-349, 1987.

Rubin, A. M., Dikes vs diapirs in viscoelastic rock *Earth Planet Sci. Letters*, v. 119, 641-659, 1993.

Rubin, A. M., Propagation of magma filled cracks, *Ann. Rev. Earth Planet.Sci*, 23, 287-336, 1995.

Tilling, R. I., Fluctuations in surface height of active lava lakes during the 1972-1974 Mauna Ulu eruption, Kilauea volcano, Hawaii, *J. Geophys. Res*, 92, 13,721-13,730, 1987.

Thornber, C. R., Kilauea's ongoing eruption; Napau Crater revisited after 14 years, (abstract), American Geophysical Union, *EOS*, Vol. 78, no. 17 Suppl. p. 329, 1997.

Wilson, L. and J.W. Head, Ascent and eruption of basaltic magmas on the earth and moon, *J. Geophys. Res*, 86, 2971-3001, 1981.

Zumberge, J. F., Heflin, M. B., Jefferson, D. C., Watkins, M. M., and Webb, F. H., Precise point positioning for the efficient and robust analysis of GPS data from large networks *J. Geophys. Res*, 102, 5005-5017, 1997.

Paul Segall, Department of Geophysics, Stanford University, Stanford, CA 94305. (e-mail: segall@stanford.edu)

Received ????; revised ????; accepted ????.

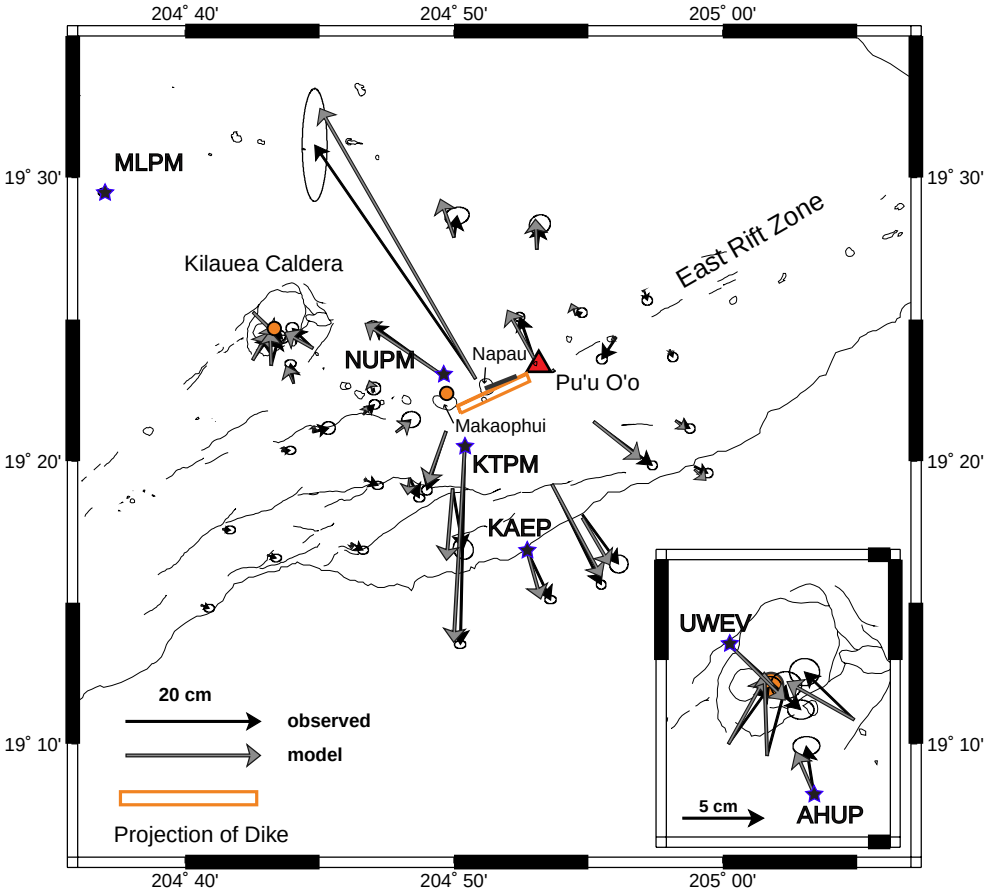

Figure 1. Location map showing the 1997 fissures, the map projection of the dike inferred from the inversion of geodetic observations (rectangle) from *Owen et al.,* [2000a]. The location of the continuously recording GPS stations referred to in the text are shown by stars. Also shown are the observed (black) with 95% confidence error ellipses and predicted (gray) displacement vectors from a combination of permanent and campaign GPS sites. The circles mark the locations of the inferred centers of deflation. The inset shows a close-up of the Kilauea summit region.

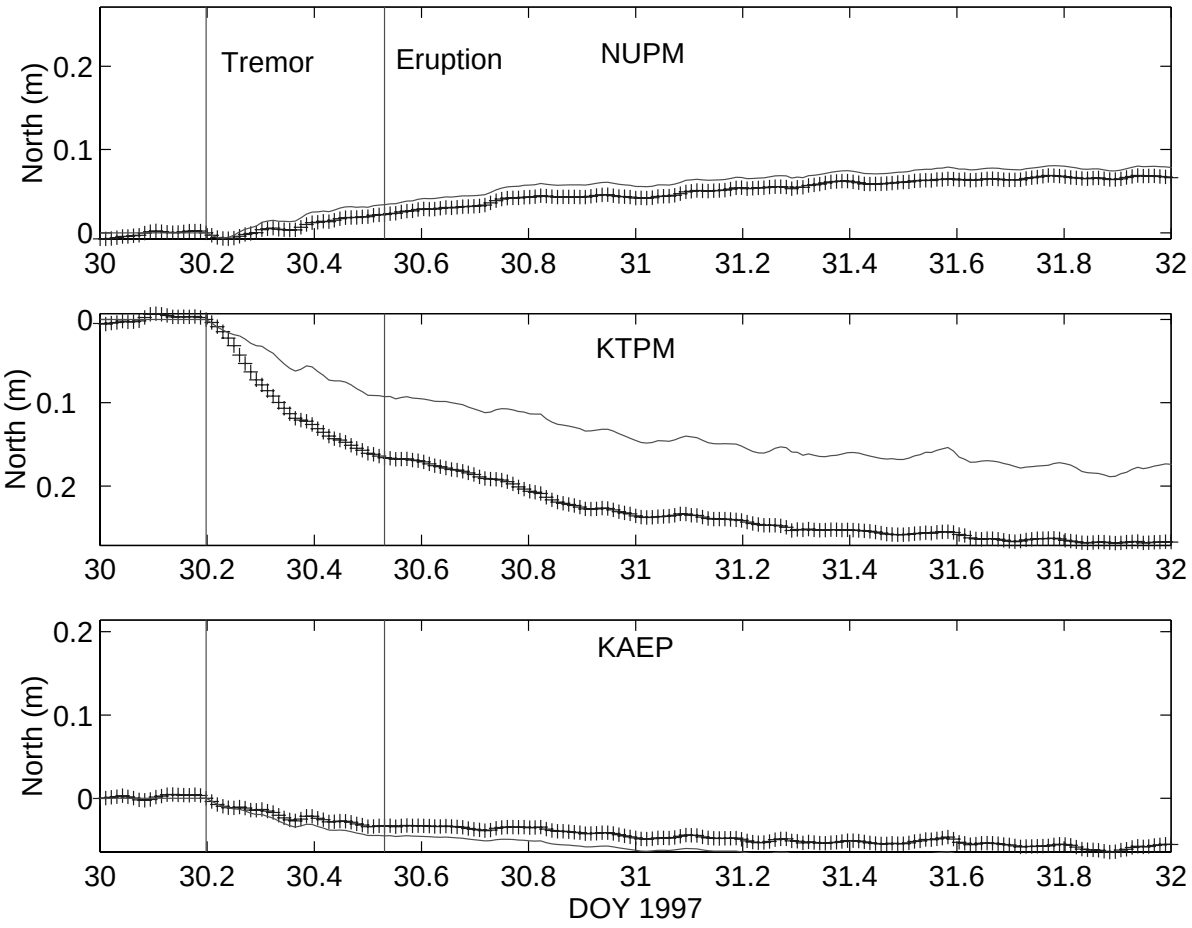

Figure 2. North component of displacement for continuous GPS stations relative to station MLPM on Mauna Loa. (a) NUPM (b) KTPM (c) KAEP. The data are shown as pluses and the predictions of a simple time varying dike model are shown as the solid curve. The observational errors follow a Gaussian random walk, equivalent to fitting the time derivative of the observations. The first vertical line marks the time of tremor onset, the second vertical line marks the onset of the eruption.

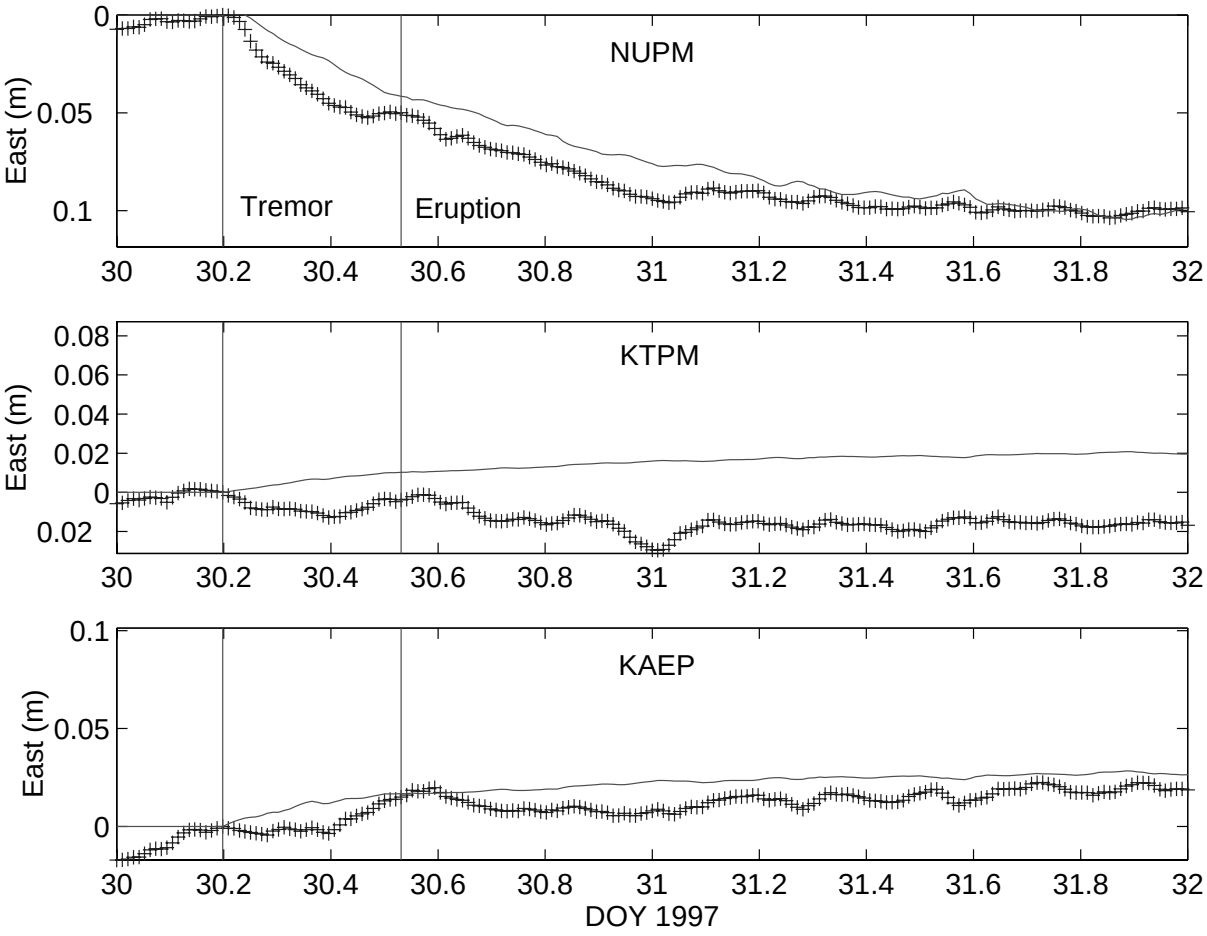

Figure 3. East component of displacement for continuous GPS stations relative to station MLPM on Mauna Loa. (a) NUPM (b) KTPM (c) KAEP. The data are shown as pluses and the predictions of a simple time varying dike model are shown as the solid curve. The observational errors follow a Gaussian random walk, equivalent to fitting the time derivative of the observations. The first vertical line marks the time of tremor onset, the second vertical line marks the onset of the eruption.

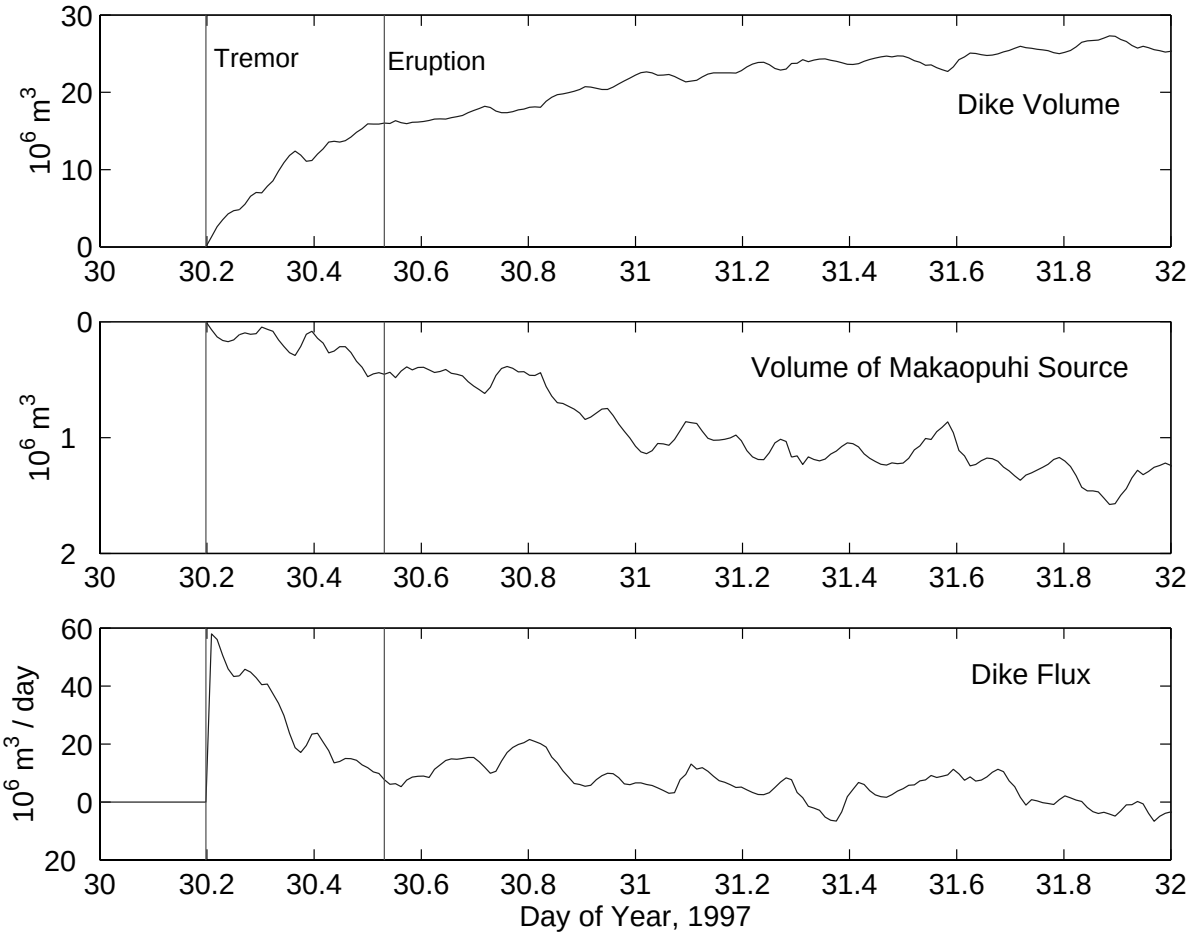

Figure 4. Dike volume history estimated from GPS data, assuming that the dike propagates vertically at a constant rate with fixed along strike dimension. The first vertical line marks the onset of harmonic tremor, the second the start of the eruption. (a) Dike volume as a function of time; (b) volume of Makaopuhi source; and (c) dike volume rate, or volume flux, from a smoothed derivative of (a).

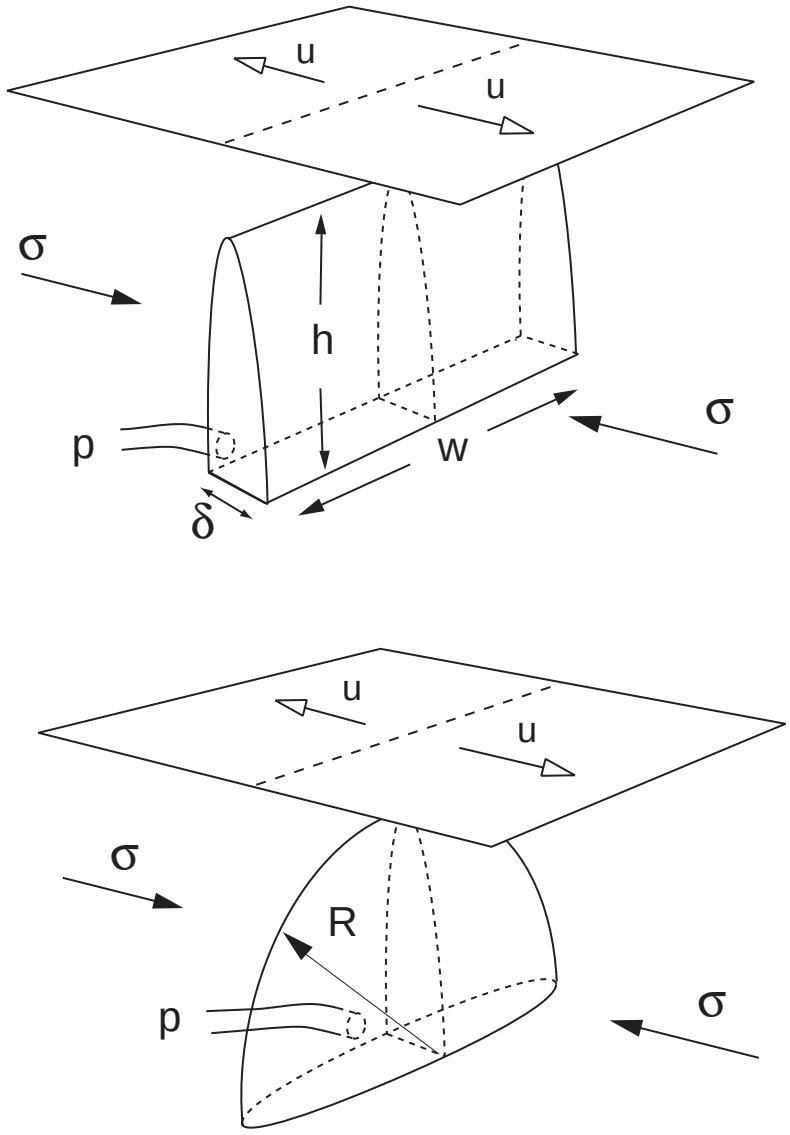

Figure 5. Geometry of a model dike propagating from depth. (a) Dike growing at fixed along strike dimension W. The dike has height h, thickness δ. The magma pressure at the dike inlet is p and the remote stress normal to the dike plane is σ. (b) An alternate model in which the dike grows radially from depth d with radius R.

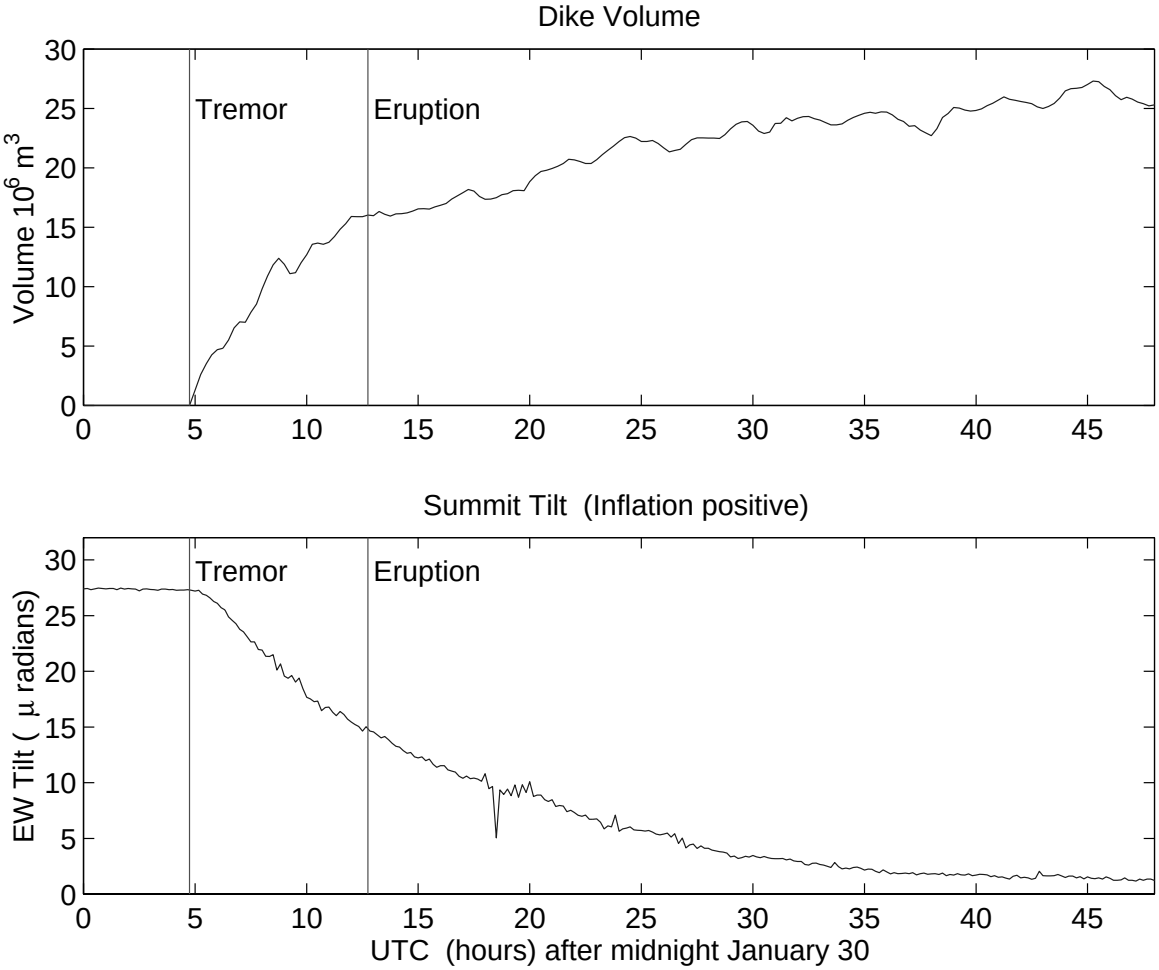

Figure 6. Comparison of estimated dike volume history with tilt record at Kilauea summit. (a) Dike volume history from Figure 15a. (b) Uwekahuna tilt at Kilauea summit. Plot shows E-W tilt in microradians with positive tilt indicating inflation of the summit magma chamber. Time axis is in hours (UTC) after midnight January 30, 1997.

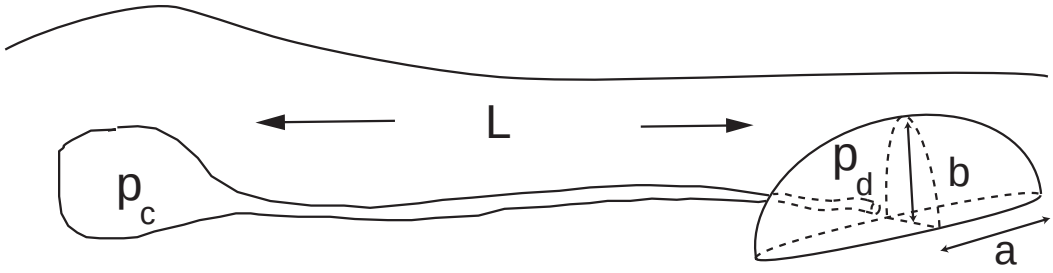

Figure 7. Geometry of the coupled magma chamber dike system. The chamber with magma pressure p_c is connected to the dike through a conduit of length L. Pressure at the dike inlet is p_d. The dike is modeled as a semi-ellipsoid with along strike semi-major axis a and height b.

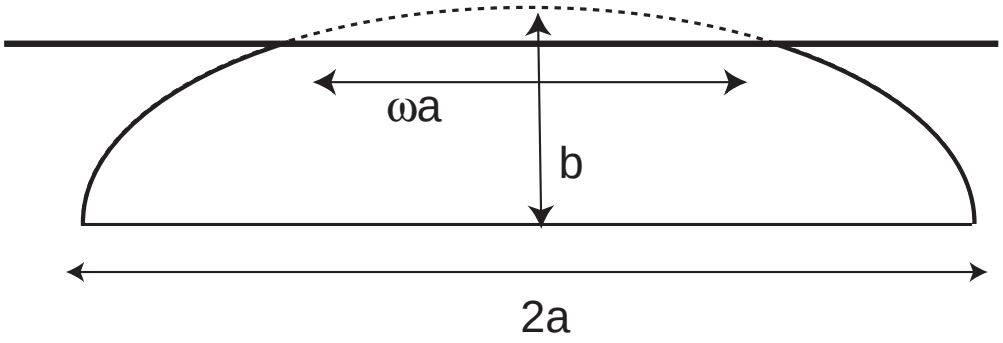

Figure 8. Definition of the eruptive fissure length ωa. If the dike height b exceeds the depth d, the dike is erupting, and the chord ωa can be taken as a measure of the eruptive fissure length.

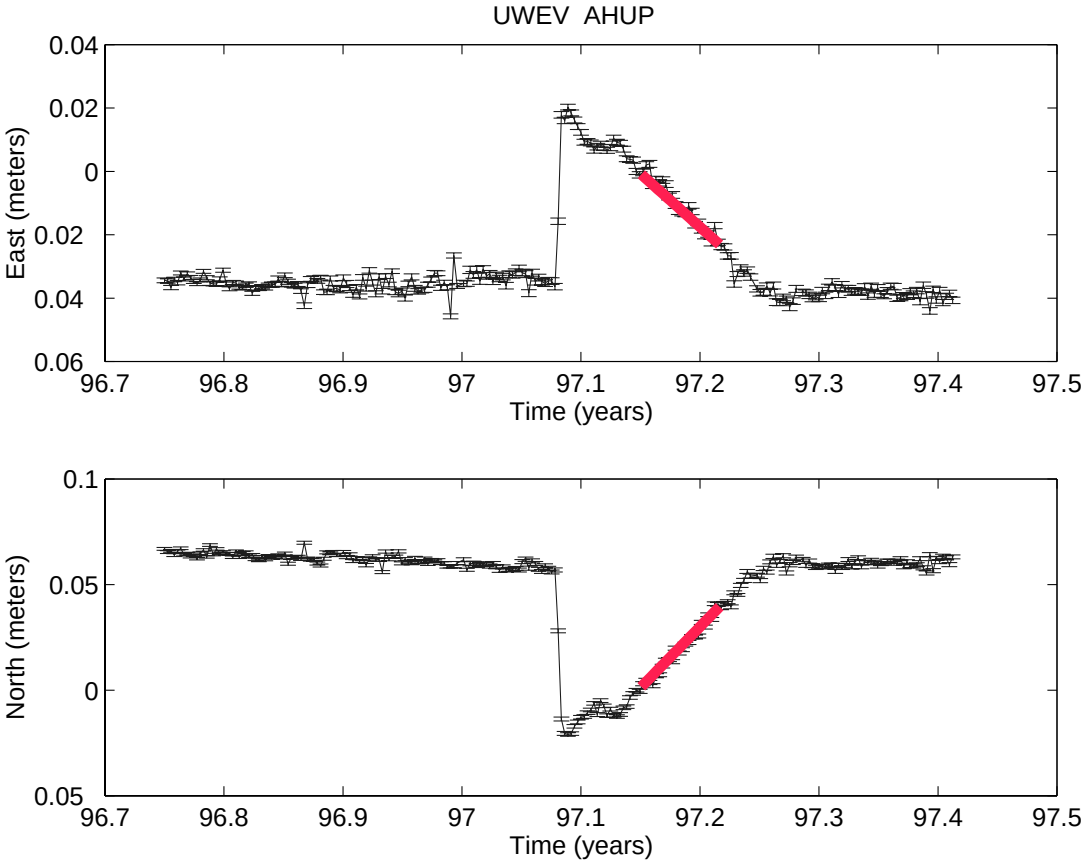

Figure 9. East (a) and North (b) components of the baseline between AHUP and UWEV. Each point with one sigma error bars represents one day position determination from the permanent GPS stations. The rapid south and east motion of UWEV with respect to AHUP marks deflation coincident with the January 30, 1997 eruption at Napau Crater. The steady westward and northward motion between February and March, 1997 marks inflation of the summit magma chamber. Straight lines indicate least squares fits to the data between February 24 and March 21, 1997, assuming steady-state inflation and a point center of inflation at a depth of 3 km.

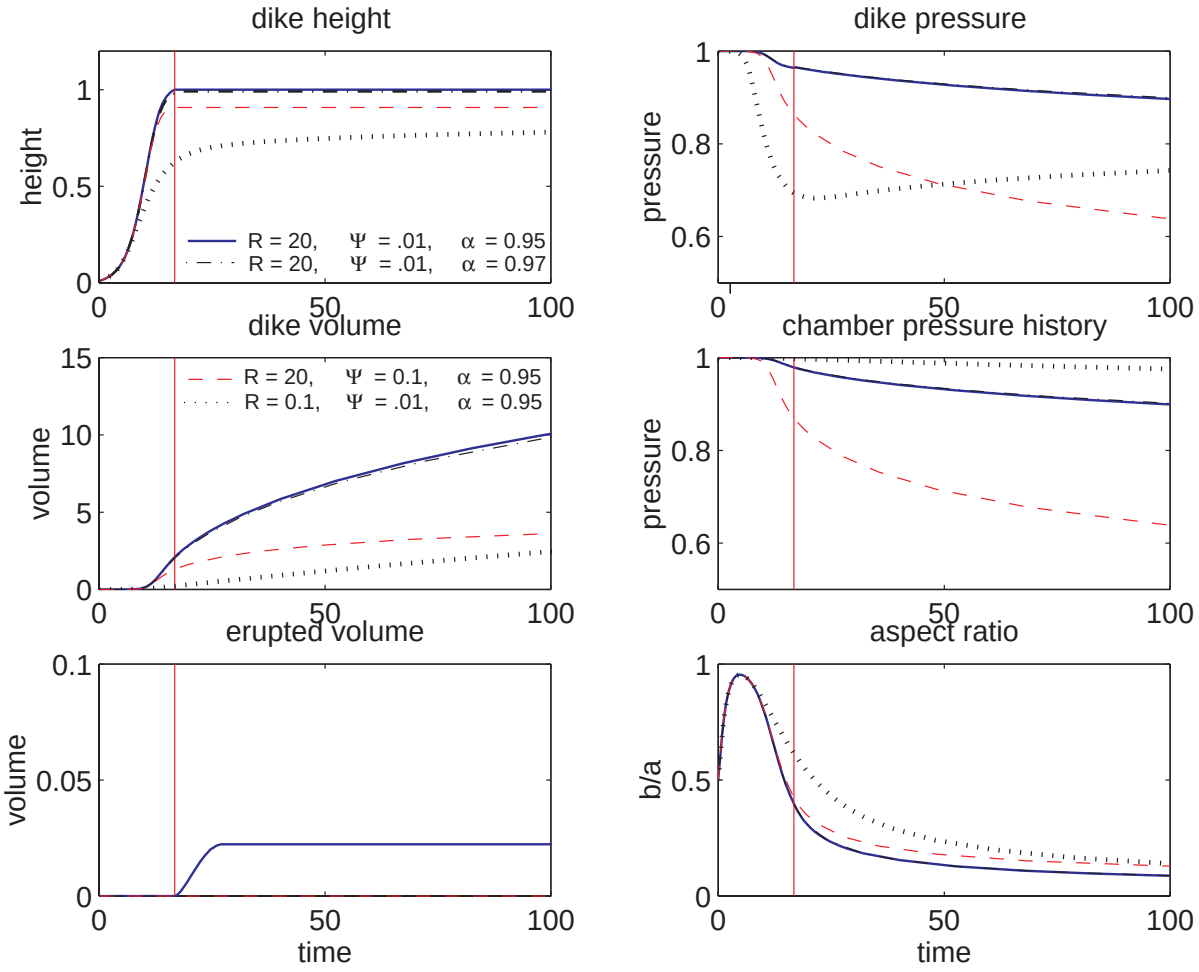

Figure 10. Simulation of the coupled dike magma chamber system for different values of $\mathcal{R}, \Psi$, and α. The panels show respectively, dike height $\tilde{h}(\tilde{t})$, dike pressure $\tilde{p}_d(\tilde{t})$, dike volume, magma chamber pressure $\tilde{p}_c(\tilde{t})$, erupted volume, and aspect ratio b/a, as a function of non-dimensional time $\tilde{t}$. All quantities are non-dimensional. Only the case $\mathcal{R} = 20$, $\Psi = 0.01$, $\alpha = 0.95$, predicts an eruption, defined as $\tilde{b} = 1$. The vertical bar marks the onset of the eruption in this case.

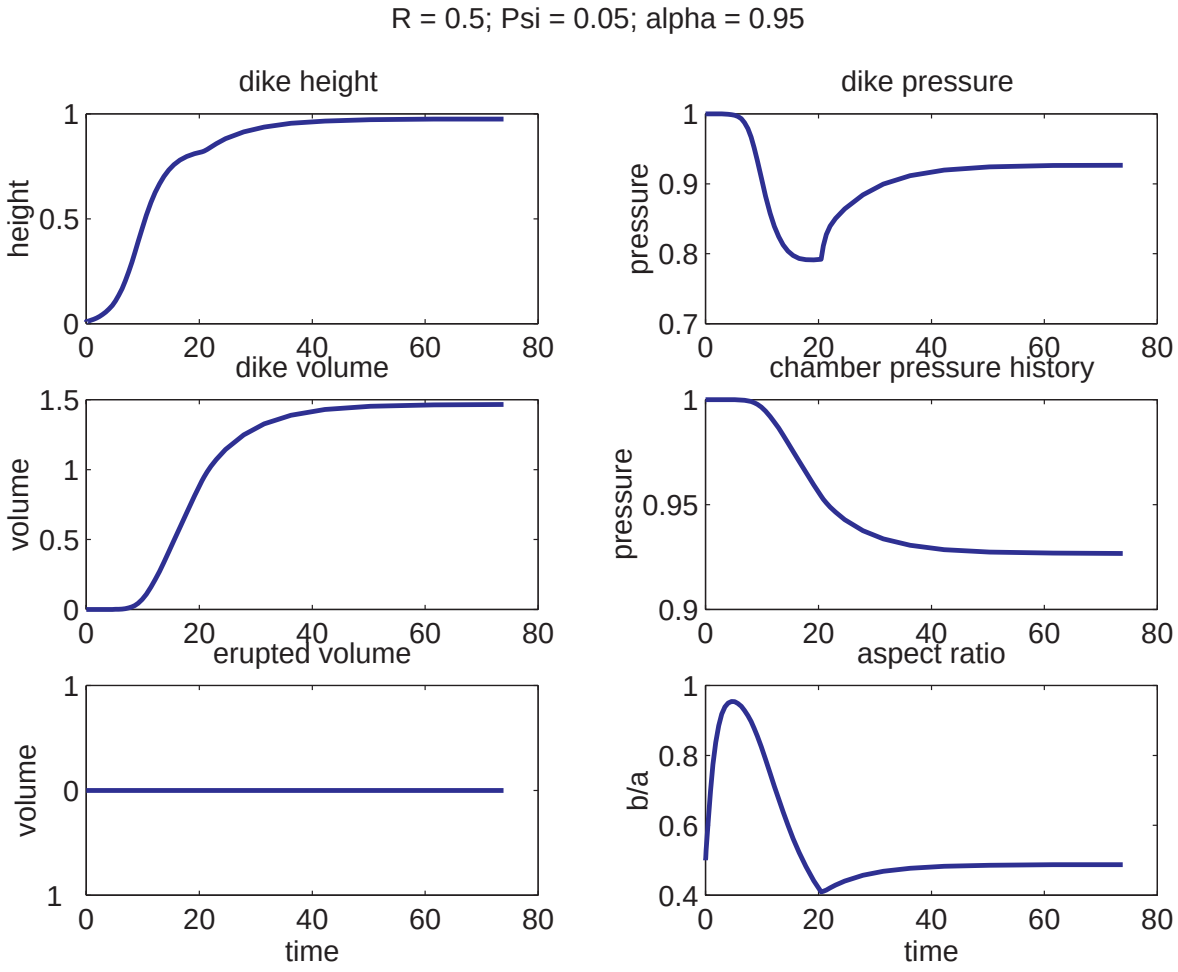

Figure 11. Simulation of the coupled dike magma chamber system for $\mathcal{R} = 0.5$, $\Psi = 0.05$, and $\alpha = 0.95$. The dike length is limited to twice the dike depth. The panels show respectively, dike height $\tilde{h}(\tilde{t})$, dike pressure $\tilde{p}_d(\tilde{t})$, dike volume, magma chamber pressure $\tilde{p}_c(\tilde{t})$, erupted volume, and aspect ratio b/a, as a function of non-dimensional time $\tilde{t}$. All quantities are non-dimensional.